Calcium Sulfate Versus PMMA in One Stage Repair of Critical-sized Femoral Defects: A Vitro Study

Yunfei Ma
Department of Orthopaedics, Nanfang Hospital
Hanjun Qin (234518319@qq.com)
Southern Medical University Nanfang Hospital
Nan Jiang
Department of Orthopaedics, Nanfang Hospital
Zilong Yao
Department of Orthopaedics, Nanfang Hospital
Qingrong Lin
Department of Orthopaedics, Nanfang Hospital
Sheng Zhang
Department of Orthopaedics, Nanfang Hospital
Yirong Chen
Department of Orthopaedics, Nanfang Hospital
Changpeng Xu
Department of Orthopaedics, The Second General Hospital of Guangdong Province
Yanjun Hu
Department of Orthopaedics, Nanfang Hospital
Yu Bin
Department of Orthopaedics, Nanfang Hospital

Research

Keywords: Induced membrane, calcium sulfate, PMMA, bone defect, Masquelet technique

Posted Date: January 13th, 2021

DOI: https://doi.org/10.21203/rs.3.rs-142241/v1

Abstract

Polymethylmethacrylate (PMMA) cement has been used in Masquelet technique to repair bone defects, but it needs additional surgery like bone grafting. This study was to compare the efficacy between PMMA and calcium sulfate (CS) used as a spacer in one-stage reconstruction of critical-sized segmental bone defects. Sprague Dawley rats (n=30) were used to create models of critical-sized femoral defect (5mm) which were then randomized into CS, PMMA and control groups equally. the bone defects were filled with CS, PMMA or nothing. Gross observation, digital radiography, histological observation and micro-computed tomography were conducted at week 20 after surgery for comparison between the three groups. The expression of Osterix, Nestin and Osteocalcin at the bone defects was also detected by immunofluorescent staining. The results of X-Ray and μCT showed that new bone formation in CS group was superior to that in PMMA group. H&E, Safranin O & fast green and Masson staining showed obvious endochondral ossification and fibrocartilage tissues at the ends of bone defects in CS group. Much more new bone tissue formed near the ends of bone defects in CS group. In addition, osteogenic and angiogenic activities were significantly increased in CS and PMMA groups. Compared with PMMA and control groups, the expression of Osteoblast-associated protein at the bone defects in CS group was higher. In general, due to the degradability of CS and superior osteogenesis ability, CS may replace PMMA as a new filling material in clinical application.

Introduction

Successful treatment of large segmental long-bone defects secondary to trauma, tumor excision, posttraumatic osteomyelitis or infected non-union remains a great challenge. It is still an unmet and urgent clinical problem how to promote repair of complicated bone defects [1]. Although bone defects up to 5 cm can be repaired with autologous, heterologous or bone graft substitutes manufactured from different materials, currently bone defects exceeding 5 cm are reconstructed by vascularized free bone graft or by Iliazarov external fixation[2]. In 1986, Masquelet developed a two-stage technique to restore wide bone loss and in 2000 introduced the induced membrane concept in an article based on his clinical results[3]. The unique biological and structural properties of the induced membrane allow bone healing almost independently in spite of the extent of the bone defect[4].

Based on the new concept, Masquelet et al. described a surgical technique combining induced membrane and subsequent autograft[3]. This procedure allows handling diaphyseal defects, longer than 25 cm, at infected, poorly vascularized and irradiated sites. The induced membrane provides an envelope that protects and revascularizes the bone graft for long bone defects at both lower and upper limbs[5, 6]. This technique is also widely used in clinical treatment of large bone defects [7].

Our previous study demonstrates that the CS-induced membranes are similar to the PMMA-induced ones in many ways. We have also found the osteo-inductivity of CS is superior to that of PMMA[8]. However, no *in vivo* experiments has shown whether CS could promote the repair of bone defects. So far there has

been no literature reporting Masquelet techniques using CS to repair bone defects. Therefore, we hypothesized that one-stage surgery using CS as a spacer could reconstruct bone defects and CS could be used in primary reconstruction of critical-sized bone defects.

Materials And Methods

Male Sprague–Dawley rats (n = 30, ten weeks old, 280–300 g, Guangzhou, Guangdong, China) were randomized into two experiment groups (CS and PMMA) and one control group. In experiment groups all rats were used to create models of critical-sized femoral defect (CSFD) which were filled with CS (Stimulan Rapid Cure, Biocomposites, Keele, U.K.) and PMMA (Simplex P, Stryker, Kalamazoo, MI), respectively. In the control group, CSFD was filled with nothing. All experiments were conducted in accordance with the regulations set by animal protection and supervision board (Project SYXK No. 2015-0056, Southern Medical University, Guangzhou, Guangdong, China). They were housed with a temperature 18–22 °C, air flow and light control (14 h day, 10 h night) and received rat food and water ad libitum. Pentobarbital sodium under general anesthesia was used throughout the operation. Before osteotomy, lidocaine was used for regional anesthesia.

Surgical procedure

After shaving and intramuscular injection of pentobarbital sodium and satisfactory anesthesia (3%, 1 ml/kg body weight), the rats were attached to an operating table with a heating blanket.

The skin, fascia, tensor fascia lata, biceps femoris, and vastus lateralis muscles of the right hind limb were incised, and the greater trochanter was elevated to expose the lateral aspect of the femur. A six-hole, 1.0 mm stainless steel mini plate (BIORTHO, Jiangsu Province, China) was applied to the lateral of the femur and fixed with proximal and distal 1.1 mm cortical screws (BIORTHO, Jiangsu Province, China). Once the mini-plate secured, CSD (critical sized defect) measuring 5 mm was fixed on the femur. Next, a high-speed power drill was used to make a critical-sized defect. The bone defects were filled with PMMA and CS cylinders (2.6 mm in diameter and 5 mm in length) respectively[9]. After local injection of lidocaine, 4 – 0 Vicryl and 3 – 0 Ethilon sutures were used to close muscle, subcutaneous and cutaneous tissues (Coated Vicryl Plus Ethicon, China). Postoperatively, the rats returned to their cages and allowed movement without restriction. Ketorolac (4 mg/kg, q24h) was used for 3 days after operation. Penicillin 20,000 IU/kg was administered intramuscularly immediately after operation, 24 and 48 hours postoperatively. After surgery, the rats were monitored for abnormal behavior and complications.

All rats were sacrificed at week 20 with overdose anesthetics administered under general anesthesia intraperitoneally.

Subsequently the rats were euthanized with an overdose of anesthetics administered intraperitoneally. Their right hindlimbs were harvested for analysis. The femurs harvested were fixed in 10% formalin solution for later μCT, paraffin embedding and immunofluorescence staining analysis.

1. Digital radiographs

Digital radiographs were taken immediately, 2, 4, 8, 12, 16 and 20 weeks post-operation under anesthesia using an Oralix AC Densomat X-ray machine (Gendex Dental System, Milan, Italy). The femurs were harvested at week 20 post-operation for gross observation, histological examination and μCT scanning.

2. Micro-computed tomography

The morphology of the reconstructed femur cortex was assessed using an animal μCT scanner (Skyscan1176, Bruker Micro-CT, Belgium). The specimens were scanned with an 80 kV energy setting, intensity of 313 μA with 280 ms acquisition time and no frame average in high-resolution mode which provided a voxel resolution of 18 μm. After μCT scan, the defect region was identified by a contour as a traced region of interest (ROI). In order to reduce CT analysis deviation caused by materials and exclude the residual material in defect area, ROI was defined as the regenerative new bone area in the 150 layers (2 mm) above at the edge of the bone defect. The relative measurements of which were calculated, including bone mineral densities (BMDs) and bone volume/total volume (BV/TV).

3. Histochemistry and immunohistochemistry analysis of bone defects

The rats were euthanized at week 20 after implantation of CS, PMMA or nothing (control group), respectively. The harvested femur samples were fixed with 4% neutral buffered formalin (NBF) for 2 days first. After μCT scanning, the samples were decalcifed in 10% EDTA (pH 7.4) for 12 weeks and dehydrated in graded ethanol (70–100%). Finally, they were embedded in paraffin and cut in 6 μm thick sections using a microtome for staining. Hematoxylin & Eosin (H&E) staining, Safranin O & fast green staining and Masson's Trichrome staining were utilized according to the manufacturer's protocols to distinguish cells from surrounding connective tissues. For immunohistochemical staining, we used a horseradish peroxidase-streptavidin detection system (Dako). Then the observer who was blinded to the conditions of the specimens used low and high magnifications with an Optiphot-2 (Olymbus@) photomicroscope. For immunofluorescence staining, second antibodies conjugated with fluorescence were incubated for 1 h at room temperature (RT) while avoiding light. Quantitative analysis was conducted in a blinded fashion with software image J (ImageJ 1.51j8). The number of positively stained cells was counted in the whole bone defect area per specimen and five sequential specimens per mouse in each group were measured.

4. Statistical analysis

All data collected were reported as means with standard deviations and P values ≤ 0.05 defined as statistically significant differences. For normally distributed data, Student t test or one-way analysis of variance (ANOVA) was used to compare differences between 2 different groups or among more than 2 groups. All statistical analyses were performed using SPSS 13.0 software (SPSS Inc, Chicago, IL, USA).

Results

1) General observation and radiographic analysis of bone defects

The stabilized femur bone defects (2.6 mm × 5 mm, diameter × length) were filled with CS/PMMA cement and the wounds closed(Fig. 1A-D). The gross appearance of the samples harvested at week 20 postoperation showed healing of bone defects in CS group while partial bone healing and some bone defects were seen in PMMA group. In the control group, no significant changes were observed in the bone defect regions (Fig. 1E-G).

The tracked X-ray radiographs are shown in Fig. 2. As presented in figure, both CS and PMMA were radiopaque so that the bone substitute filled in the bone defects was visible. At week 8 postoperation, resorption of almost all CS was shown because the images became blurred at the bone defects and the CS was hard to note. We also found formation of the membrane around the CS area (Fig. 2 C). At week 20 postoperation, we found union of bone defects (Fig. 2F). In PMMA group, the material in the bone defect showed no noticeable degradation (Fig. 2G-L). In the empty control group, bone defect regions also showed no significant changes compared with previous ones (Fig. 2 M-R).

2) Micro-CT measurement

The morphology of the newly formed bone was was evaluated using Micro-CT. 3D microarchitecture of the bone defect area was evaluated. The μCT cross sections of the defect area showed more obvious new bone formation in CS group (Fig. 3A-B) than in PMMA group (Fig. 3 C-D).

Compared with the control group (Fig. 3E-F), CS and PMMA groups exhibited greater new bone formation but incomplete cortex and voids beneath the cortex (Figs. 3).

The quantity of the newly formed bone at the defect sites was calculated by morphometric analysis (Fig. 3G-H). The data concerning BMDs and mean BV/TV percentage demonstrated significantly more BMDs at the defect sites in CS group than in PMMA and control groups at week 20 postoperatively.

3) Histological analysis of bone defects

CS group. At week 20 postoperation, the borders of bone defects were stained with H&E, Safranin O & fast green and Masson staining (Figs. 4A, D and G). Much more new formed bone tissue was observed adjacent to the borders. However, also observed were endochondral ossification and newly formed fibrous cartilage, even a fibrous connection formed by mature lamellar bone around the bone defects.

PMMA group. At 20th week postoperatively, the borders of bone defects were stained with H&E, Safranin O & fast green and Masson staining (Figs. 4B, E and H). Endochondral ossification and newly formed fibrous cartilage were observed but no fibrous connection formed at the bone defect area.

Control group. At 20th week postoperatively, the borders of bone defects were stained with H&E, Safranin O & fast green and Masson staining. Many capillaries and a small amount of neutrophils, monocyte,

fibroblasts, myofibroblasts, collagen and newly formed fibrous cartilage were observed (Figs. 4 C, F and I).

4) Expression of Nestin, Osteocalcin (OCN) and Osterix (OSX)at bone defects area

The immunofluorescent staining and quantitative analysis expression showed that the expression of $Osterix^+$ cells, $Nestin^+$ cells and $Osteocalcin^+$ cells at the edge of the bone defect in CS group was significantly higher than that in PMMA and control groups (Figs. 5–7). All these indicated that the osteogenesis ability of CS group was significantly stronger than that of PMMA group and control group.Compared with the PMMA combined control group, the CS group had better bone defect repair ability.

4) Expression of Runx2 at bone defects area

We used immunohistochemical staining to detect the expression of Runx2-positive cells between groups at the edge of the bone defect.RUNX2 is an important marker for bone formation. As can be seen from Fig. 8, the CS group contained a large number of Runx2-positive cells in the edge of bone defect, which was much higher than the PMMA group and the control group.We used immunohistochemical staining to detect the expression of RUNX2 positive cells between groups at the edge of the bone defect.RUNX2 is an important marker for bone formation. As can be seen from Fig. 8, the CS group contained a large number of Runx2-positive cells in the edge of bone defect, which was much higher than the PMMA group and the control group. There were only a few Runx2-positive cells in the PMMA group and almost no runx2-positive cells in the control group, which was consistent with the results of new bone formation around bone defects in each group.

5) Expression of H-type vessel at bone defects

As in previous studies, high expression of endothelial markers CD31 and Emcn (CD31hiEmcnhi) were used to label h-type vessels in immunofluorescence staining. We can clearly observe that the H-type vessels in the CS group are significantly more than those in the PMMA group and the control group(Figure 9).This means that in the bone defect area, the CS group has a better vascular environment to promote new bone formation.

Discussion

In current clinical practice, the duration varies from 6 weeks to 9 months between the first surgery when PMMA cement is placed into a defect and the secondary surgery when the membrane is opened and the cement is replaced with autologous bone graft. It is reported that complete bone healing and functional recovery (weight bearing) is achieved at 3–9 months after the secondary operation[10, 11]. Our previous rat model of femoral segments revealed that the maximal neovascularization and osteogenic activity

occurred at 6th week[8]. This study has demonstrated that CS can be used in one-stage reconstruction of critical-sized femoral defects, sparing surgical removal of the spacer. In CS-group, the induced membrane may act as a bioreactor, concentrating growth factors or regenerative cells locally to the defect zone to promote healing of bone defects.

Critical bone defects (CSD) refer to those that cannot reach the critical point of bone healing in a natural state to a certain extent[12, 13]. When a long bone defect reaches 1.5 times of its diameter, it can be considered as a CSD[14, 15]. At present, the Masquelet technique has become one of the important treatments for CSDs.

The induced membrane by Masquelet technique contains a high-density microvascular system which can secrete VEGF, TGF-β1 and other growth factors to promote bone formation[16, 17]. Therefore, improving the biological activity of the induced membrane and accelerating the micro-vascularization of the induced membrane can lay a foundation for later bone reconstruction.

Despite the notable benefits of the Masquelet procedure, some flaws must be kept in mind[18]. Graft harvesting could cause direct complications on donor site that should have been included in the pitfalls of induced membrane technique [19]. Complications due to iliac crest bone harvesting include fractures of the iliac wing or superior iliac spine and hematoma (higher if the harvesting is on the anterior iliac crest) and infection. It can also cause long-lasting donor site pain, injuries to vessels and nerves and a scar cosmetically unaccepted [20].

PMMA cement, introduced by Buchholz and Engelbrecht in 1970 for localized antibiotic delivery, is a spacer widely used because of its benefits of being able to bear weight and variable antibiotic elution rates. It also bears such disadvantages as limited antibiotic release, incompatibility with many antimicrobial agents, and necessity of a secondary surgery for residual cement removal prior to surgical reconstruction of a bone defect[21, 22]. Therefore, extensive research pursuits are targeting alternative, biodegradable materials to replace PMMA, like CS [22, 23].

In animal experiments, we compared the efficacy of CS group, PMMA group and control group in the treatment of critical bone defect through the construction of rat bone defect model. It was found that CS was significantly superior to PMMA in membrane induction and osteogenesis, and had good degradability.

In this study, we have demonstrated that CS can repair a critical bone defect at one stage. In CS group, induced membrane formed around a bone defect within 8 weeks. With time the tissue of induced membrane was gradually absorbed, promoting healing of the bone defect at 20 weeks postoperation. Partial bone union was seen around the bone defect in PMMA group, indicating PMMA can also promote formation of osteoblasts. However, because PMMA is not degradable, it will hinder the healing of a bone defect. At the same time, we found that the CS group had a better osteogenic effect.It can effectively promote the recruitment and osteogenic differentiation of bone marrow mesenchymal stem cells.

Although the identity of MSCs is still not straightforward, Nestin$^+$ cells in the bone marrow have been shown to represent a subset of bone marrow precursor cells mainly in endothelial cell lineage and mesenchymal lineage. Moreover, Nestin$^+$ cells are major osteoblast-forming mesenchymal stromal precursor cells (MSPCs) in adult bone marrow[24].

In our study, a large number of Nestin positive cells were observed in the bone defect of CS group, while only a small number of Nestin positive cells were observed in PMMA group, and even fewer Nestin positive cells were observed in the control group. It is well known that the number of bone marrow mesenchymal stem cells(BMSCs) is important for bone formation. In the CS group, there are more BMSCs around the bone defect, which means that CS has a more significant recruitment effect on BMSCs, and also has a greater promotion effect on membrane induced bone formation. OCN and OSX, osteoblast specific genes, are considered to be the main regulatory genes in bone formation. Expression of OCN and OSX plays an important role in the differentiation of stem cells into osteoblasts[25]. Osx, one of the structural specific genes in osteoblasts, regulates the expression of many important osteogenic phenotypes and functional proteins[25, 26]. It was reported that in a mouse embryos with OSX gene removed, the expression levels of various osteogenic differentiation markers were severely reduced or absent and the differentiation and maturation of osteoblasts were completely blocked. OCN, a specific product of osteoblast differentiation, mainly occurs during mineralized formation, reflecting the activity of osteoblasts and bone transformation level[27].In the experiment, we found that CS group had significantly superior osteogenesis compared with the other two groups, and the bone defect edge also presented higher level of OST and OCN. In addition, the immunohistochemical results of another osteogenic marker, RUNX2, were also highly consistent with OST and OCN. Interestingly, we found that the H-type vessel was significantly overexpressed in the CS group.Previous studies have found that h-type blood vessels, characterized by high expression of endothelial markers CD31 and Emcn (CD31hiEmcnhi), generate a unique microenvironment to maintain perivascular bone progenitor cells and link angiogenesis to bone progenitor cells, a specific blood vessel that clearly promotes bone formation[28]. It suggests that CS has better membrane induction and osteogenesis ability, which may be related to the promotion of angiogenesis.

In this study, we found that CS has a better therapeutic effect than PMMA in Masquelet technique and may become a substitute for PMMA. However, this study still has certain limitations. Firstly, although a large number of experimental results in this study support that CS has superior osteogenesis ability in Masquelet technique compared with PMMA, the specific signal mechanism is still unclear. Secondly,we mainly observed a one-stage repair of bone defects and did not perform a staged surgery and the functional improvements were not quantitatively assessed in this study. Further experiments are required.

Conclusion

The present results suggest that CS has a potential to replace PMMA as a spacer for a bone defect in the Masquelet technique. This might lead to a better and faster healing of a critical-sized bone defect,

benefiting the patients concerned.

Declarations

Ethics approval and consent to participate

All experiments were conducted in accordance with the regulations set by animal protection and supervision board (Project SYXK No. 2015-0056, Southern Medical University, Guangzhou, Guangdong, China).

Consent for publication

All authors reviewed and agreed upon the manuscript. All authors agree to publish the article.

Availability of data and material

We declared that materials described in the manuscript, including all relevant raw data, will be freely available to any scientist wishing to use them for non-commercial purposes, without breaching participant confidentiality.

Acknowledgment

Not applicable.

Authors' contributions

Bin Yu and Yanjun Hu conceived and designed the experiments. Yunfei Ma and Hanjun Qin performed the experiments. Yunfei Ma , Hanjun Qin and Nan Jiang wrote the manuscript. Hanjun Qin, Zi-long Yao, Qing-rong Lin Sheng zhang, Yi-rong Chen and Chang-peng Xu analyzed the data and prepared all the figures. All authors reviewed and agreed upon the manuscript.

Funding

The study was supported by National Natural Science Foundation of China (81830079 and 81972083) and China Postdoctoral Science Foundation Grant (2018M633075). Science and Technology Program of Guangzhou（202002020001）.

Competing interests

The authors declare that they have no conflict of interest concerning this article.

References

[1] Ball AN, Donahue SW, Wojda SJ, et al. The challenges of promoting osteogenesis in segmental bone defects and osteoporosis [J]. J Orthop Res, 2018, 36(6): 1559-72.

[2] Giannoudis PV, Faour O, Goff T, et al. Masquelet technique for the treatment of bone defects: tips-tricks and future directions [J]. Injury, 2011, 42(6): 591-8.

[3] Masquelet AC, Fitoussi F, Begue T, et al. [Reconstruction of the long bones by the induced membrane and spongy autograft] [J]. Ann Chir Plast Esthet, 2000, 45(3): 346-53.

[4] Han W, Shen J, Wu H, et al. Induced membrane technique: Advances in the management of bone defects [J]. Int J Surg, 2017, 42(110-6.

[5] T Z, X G, A A, et al. [Induced membrane technique for the reconstruction of bone defects in upper limb. A prospective single center study of nine cases] [J]. Chirurgie de la main, 2011, 30(4): 255-63.

[6] Td L, Fa N, Aa L, et al. Management of recalcitrant osteomyelitis and segmental bone loss of the forearm with the Masquelet technique [J]. The Journal of hand surgery, European volume, 2017, 42(6): 640-2.

[7] C M, Me H, V C, et al. Reconstruction of Long Bone Infections Using the Induced Membrane Technique: Tips and Tricks [J]. Journal of orthopaedic trauma, 2016, 30(6): e188-93.

[8] Ma YF, Jiang N, Zhang X, et al. Calcium sulfate induced versus PMMA-induced membrane in a critical-sized femoral defect in a rat model [J]. Sci Rep, 2018, 8(1): 637.

[9] Henrich D, Seebach C, Nau C, et al. Establishment and characterization of the Masquelet induced membrane technique in a rat femur critical-sized defect model [J]. J Tissue Eng Regen Med, 2013,

[10] T A, N B, P C, et al. Two-stage reconstruction of post-traumatic segmental tibia bone loss with nailing [J]. Orthopaedics & traumatology, surgery & research : OTSR, 2010, 96(5): 549-53.

[11] Powerski M, Maier B, Frank J, et al. Treatment of severe osteitis after elastic intramedullary nailing of a radial bone shaft fracture by using cancellous bone graft in Masquelet technique in a 13-year-old adolescent girl [J]. J Pediatr Surg, 2009, 44(8): E17-9.

[12] Clough BH, Mccarley MR, Gregory CA. A simple critical-sized femoral defect model in mice [J]. J Vis Exp, 2015, 97):

[13] Kerzner B, Martin HL, Weiser M, et al. A Reliable and Reproducible Critical-Sized Segmental Femoral Defect Model in Rats Stabilized with a Custom External Fixator [J]. J Vis Exp, 2019, 145):

[14] Cm B, E B, Mr M. Comparative bone anatomy of commonly used laboratory animals: implications for drug discovery [J]. Comparative medicine, 2011, 61(1): 76-85.

[15] M P, I D-C, D G, et al. The rational use of animal models in the evaluation of novel bone regenerative therapies [J]. Bone, 2015, 70(undefined): 73-86.

[16] Uk O, H E, P B, et al. The Masquelet technique of induced membrane for healing of bone defects. A review of 8 cases [J]. Injury, 2015, null(undefined): S44-7.

[17] Uzel AP, Lemonne F, Casoli V. Tibial segmental bone defect reconstruction by Ilizarov type bone transport in an induced membrane [J]. Orthop Traumatol Surg Res, 2010, 96(2): 194-8.

[18] S C, R V, Ms O, et al. Masquelet technique and osteomyelitis: innovations and literature review [J]. European review for medical and pharmacological sciences, 2019, 23(null): 210-6.

[19] Morelli I, Drago L, George DA, et al. Masquelet technique: myth or reality? A systematic review and meta-analysis [J]. Injury, 2016, 47 Suppl 6(S68-s76.

[20] E A, M P, N R, et al. Comparison of anterior and posterior iliac crest bone grafts in terms of harvest-site morbidity and functional outcomes [J]. The Journal of bone and joint surgery American volume, 2002, 84(5): 716-20.

[21] C G, R R, Aw F, et al. The in vitro elution characteristics of antifungal-loaded PMMA bone cement and calcium sulfate bone substitute [J]. Orthopedics, 2011, 34(8): e378-81.

[22] Sj M, Rp H, J W, et al. Comparing PMMA and calcium sulfate as carriers for the local delivery of antibiotics to infected surgical sites [J]. Journal of biomedical materials research Part B, Applied biomaterials, 2015, 103(4): 870-7.

[23] Ja I, Em S, Sl K, et al. Biomaterials approaches to treating implant-associated osteomyelitis [J]. Biomaterials, 2016, 81(undefined): 58-71.

[24] Mendez-Ferrer S, Michurina TV, Ferraro F, et al. Mesenchymal and haematopoietic stem cells form a unique bone marrow niche [J]. Nature, 2010, 466(7308): 829-34.

[25] W T, Y L, L O, et al. Osteoblast-specific transcription factor Osterix (Osx) is an upstream regulator of Satb2 during bone formation [J]. The Journal of biological chemistry, 2011, 286(38): 32995-3002.

[26] Hm Z, Mj S. Proliferation and Activation of Osterix-Lineage Cells Contribute to Loading-Induced Periosteal Bone Formation in Mice [J]. JBMR plus, 2019, 3(11): e10227.

[27] Ag P, Ss H, M E, et al. Association between serum osteocalcin and markers of metabolic phenotype [J]. The Journal of clinical endocrinology and metabolism, 2009, 94(3): 827-32.

[28] Kusumbe AP, Ramasamy SK and Adams RH: Coupling of angiogenesis and osteogenesis by a specific vessel subtype in bone. NATURE 507: 323-328, 2014.

Figures

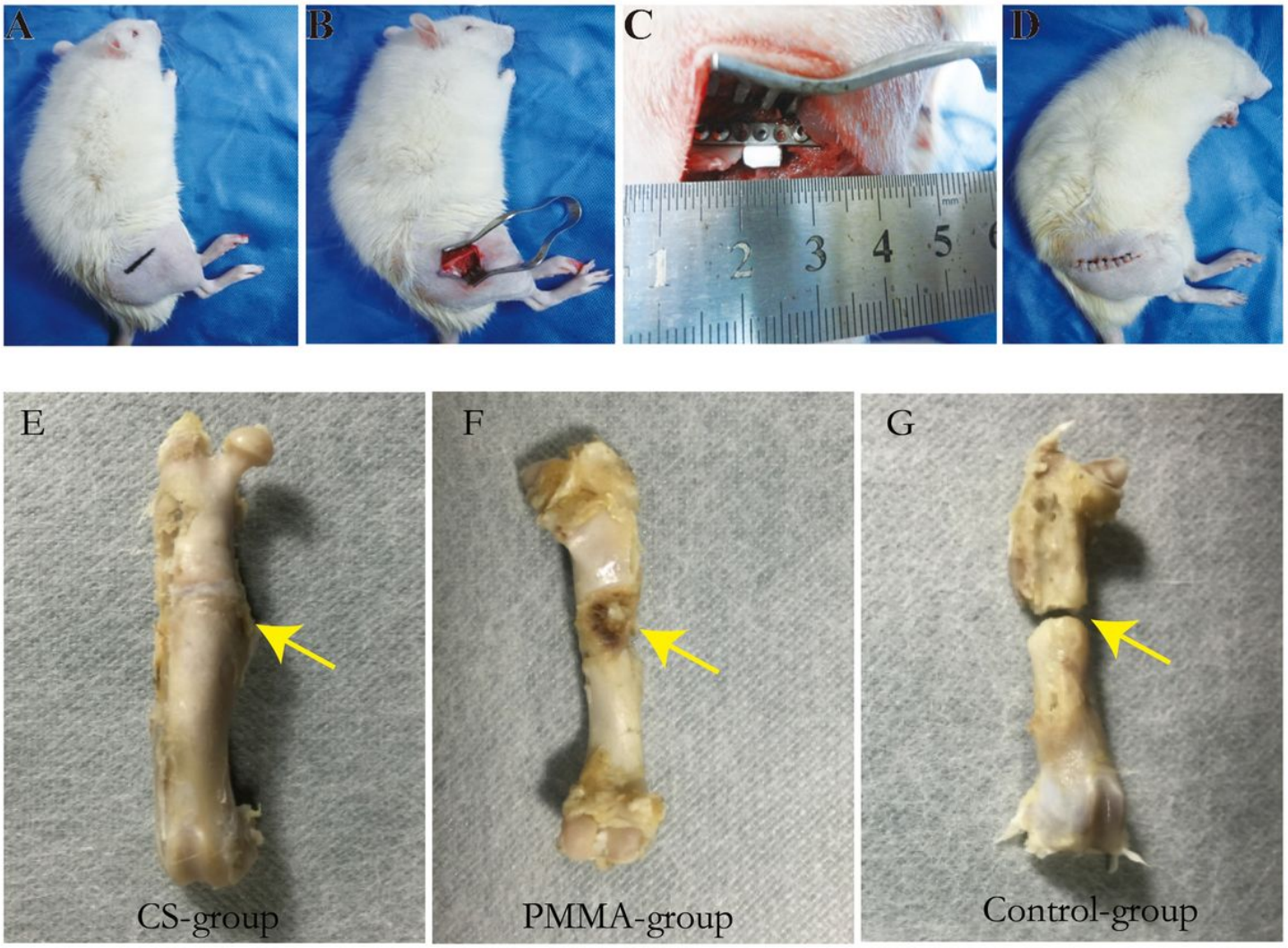

Figure 1

A stabilized femur bone defect which was filled with CS/PMMA cement and a closed wound. The size of the bone defect was φ2.6mm×5mm (diameter × length)(A-D). After 20 weeks, the animal was sacrificed and the femur was harvested. Union of a bone defect in CS group(E). In the PMMA group, bone defects were partially healed, but there were still some bone defects in the central part (F). In the control group, the bone defect was obvious (G).

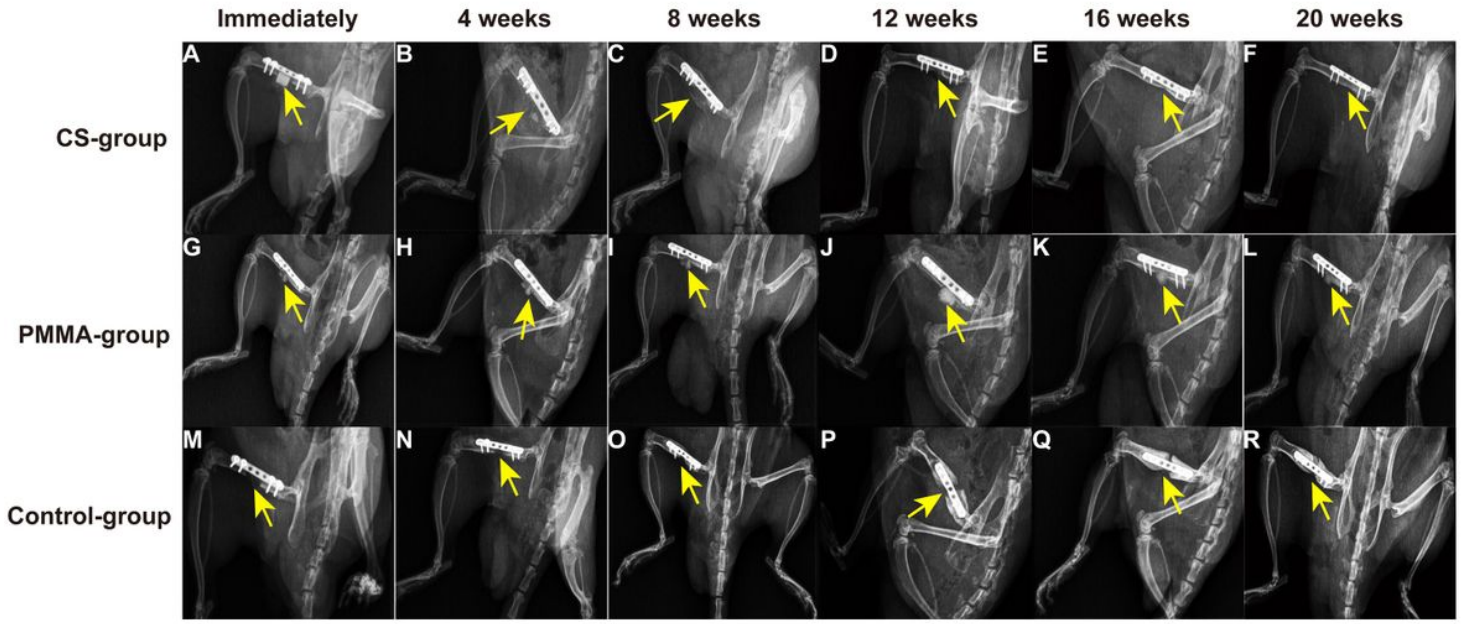

Figure 2

X-ray images of rats with a critical-sized femur bone defect in CS, PMMA and control groups, respectively. The time points were immediate postoperation, 4, 8, 12, 16 and 20 weeks postoperation. As time passing, CS was completely degraded and absorbed and the bone defect was completely healed (arrows indicate). However, there were no such significant changes in PMMA or control group.

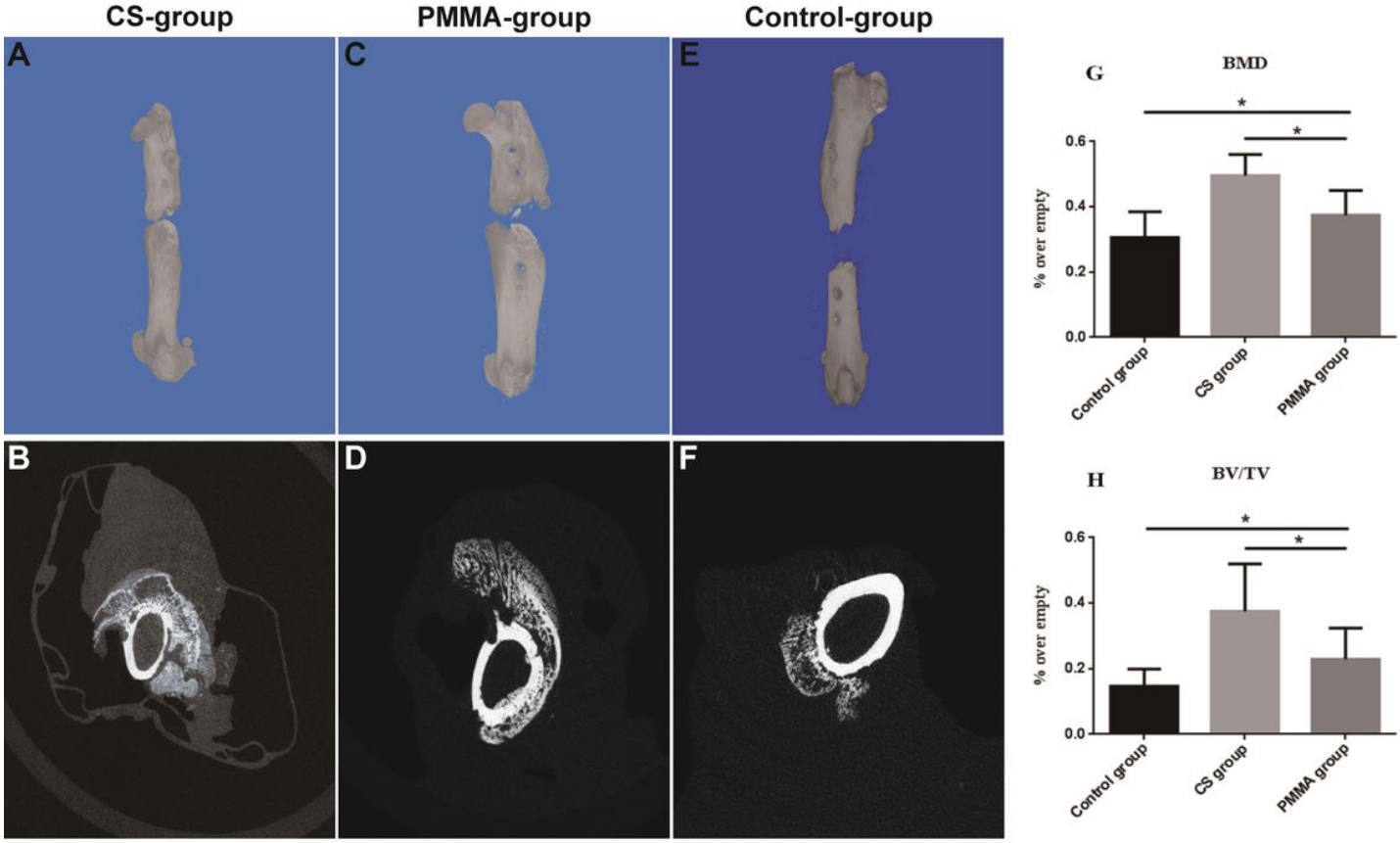

Figure 3

Morphometric evaluation of the local bone mineral densities (BMDs) and bone volume/total volume (BV/TV). PMMA group exhibited the lowest levels in both BMDs and BV/TV of the defects when compared to CS group ($P<0.05$). The control group exhibited the lowest levels in both BMDs and BV/TV of the defects when compared to CS and PMMA groups ($P<0.05$). The data further revealed that CS group had significantly more BMDs and BV/TV of the defects compared to PMMA at 20th week ($P<0.05$).

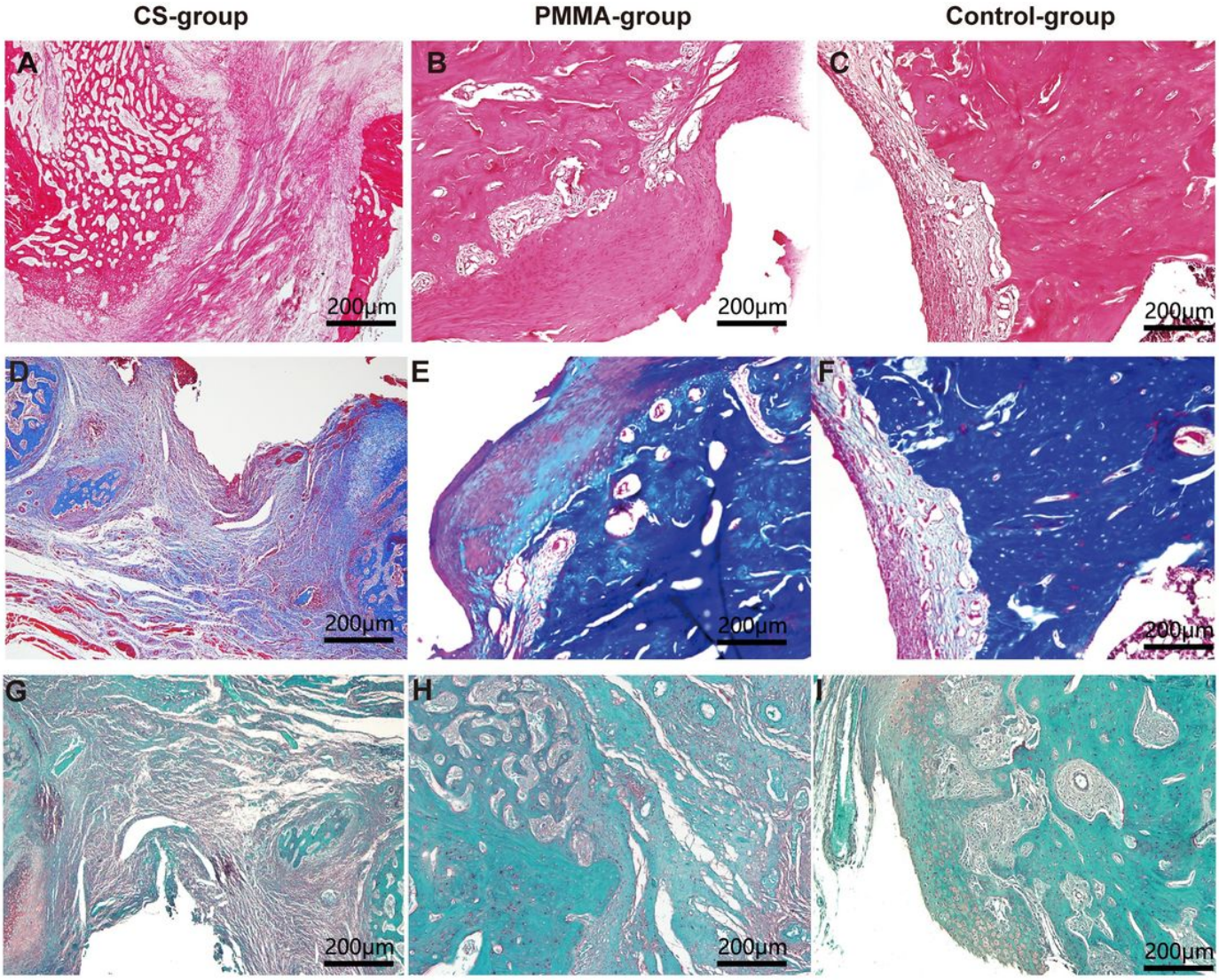

Figure 4

Representative histological sections of the bone defect ends showing the histological changes over the course of maturation of the endochondral ossification in groups(H&E staining(A-C), Safranin O & fast green staining(D-F), Masson's Trichrome staining(G-I)). A fibrous connection at the bone defect was seen in CS group. However, there was no bony connection in PMMA or control group.

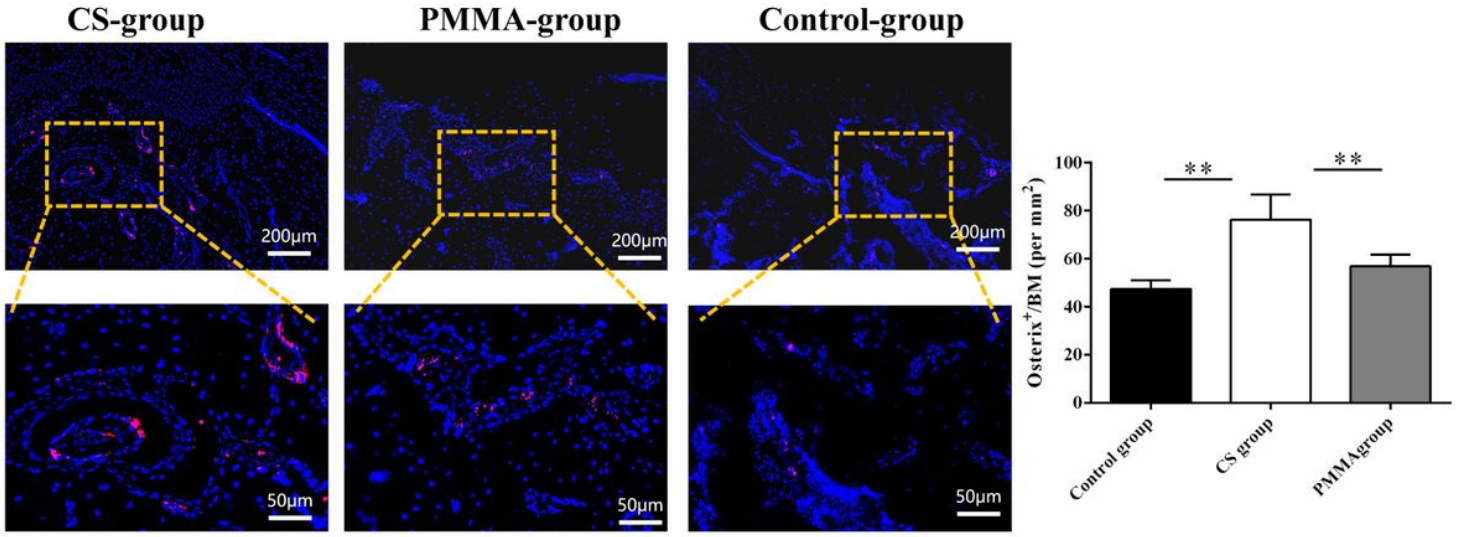

Figure 5

Immunofluorescent staining and quantitative analysis of Osterix+ cells in bone defects area at 20 weeks postoperation. n=5 per group. Scale bar, 200 μm. Magnified view, 50 μm. **p < 0.05 compared as denoted by bar.

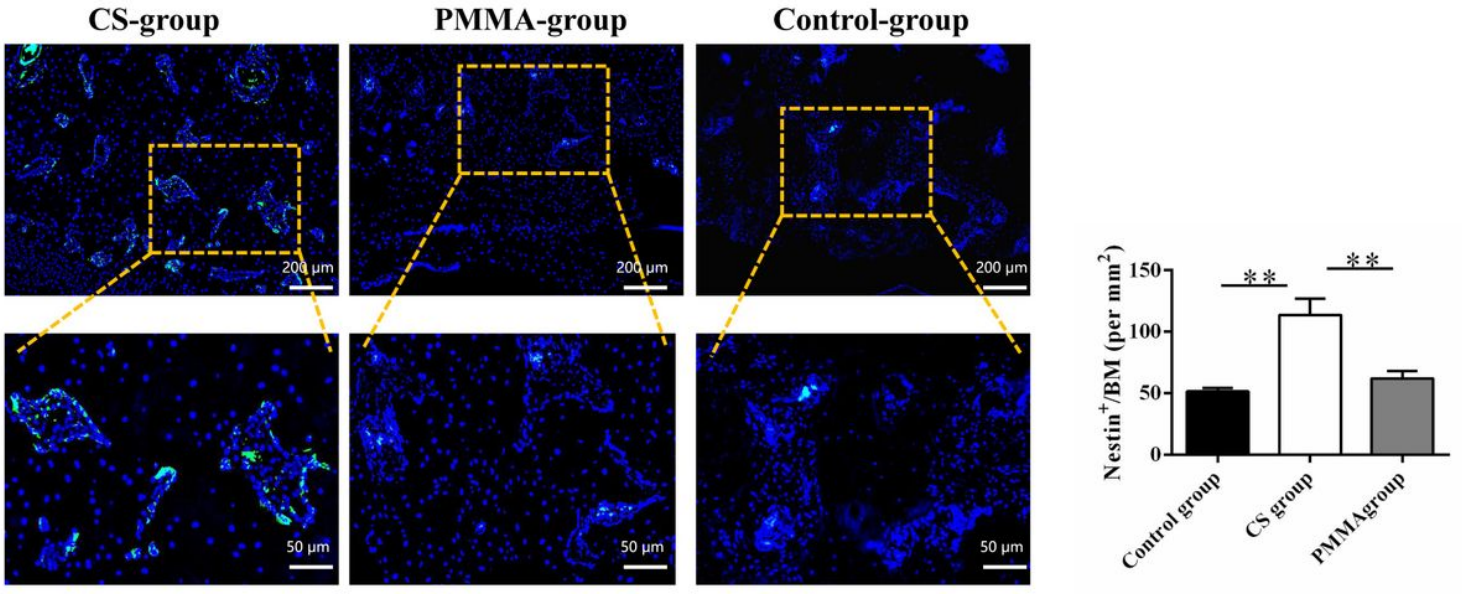

Figure 6

Immunofluorescent staining and quantitative analysis of Nestin+ cells in bone defects area at 20 weeks postoperation. n=5 per group. Scale bar, 200 μm. Magnified view, 50 μm. **p < 0.05 compared as denoted by bar.

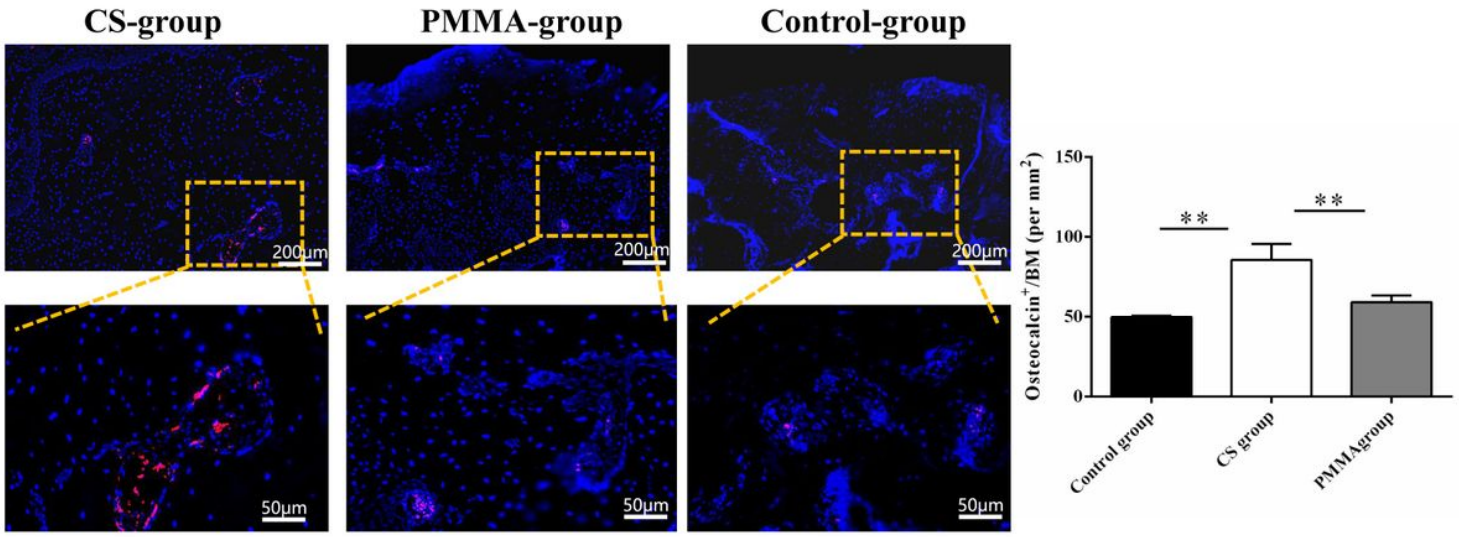

Figure 7

Immunofluorescent staining and quantitative analysis of Osteocalcin+ cells in bone defects area at 20 weeks postoperation. n=5 per group. Scale bar, 200 μm. Magnified view, 50 μm. **p < 0.05 compared as denoted by bar.

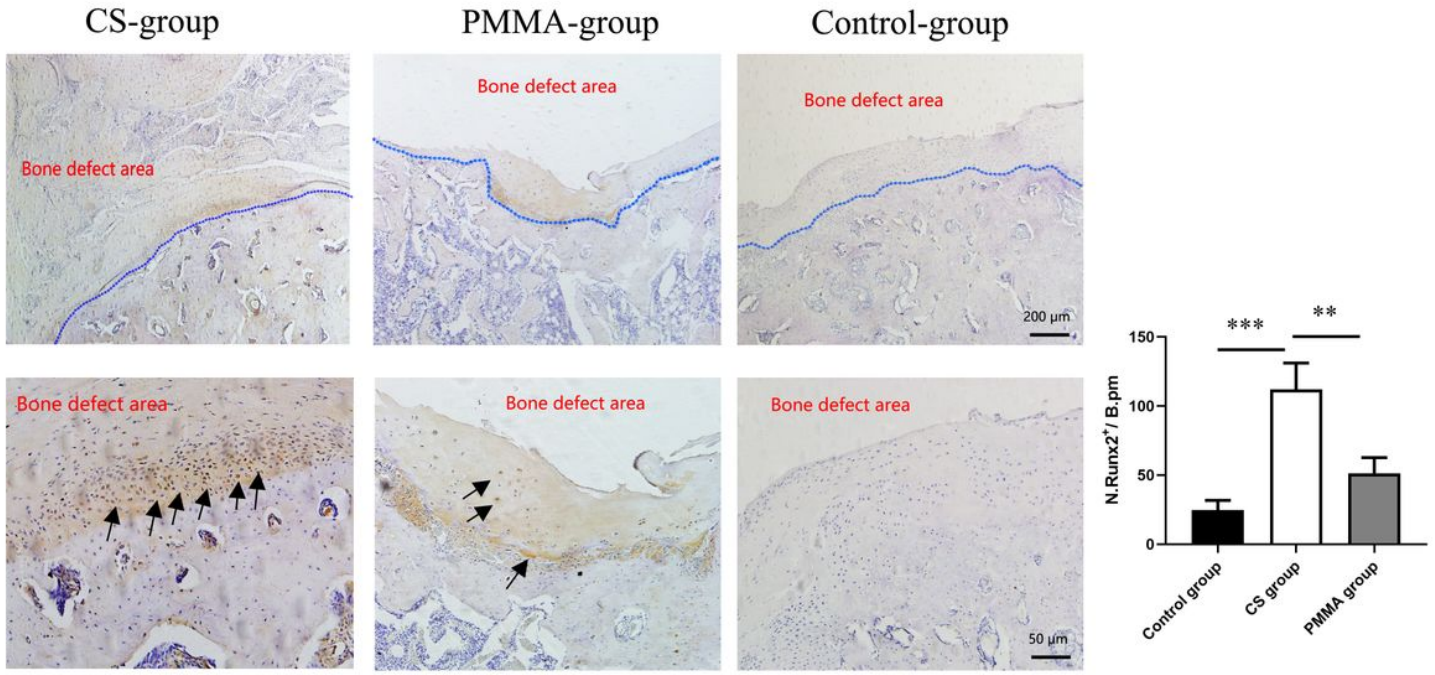

Figure 8

Immumohistochemical staining and quantitative analysis of Rnux2+ cells in bone defects area at 20 weeks postoperation. n=5 per group. Scale bar, 200 μm. Magnified view, 50 μm. **p < 0.05, ***p < 0.001

compared as denoted by bar.

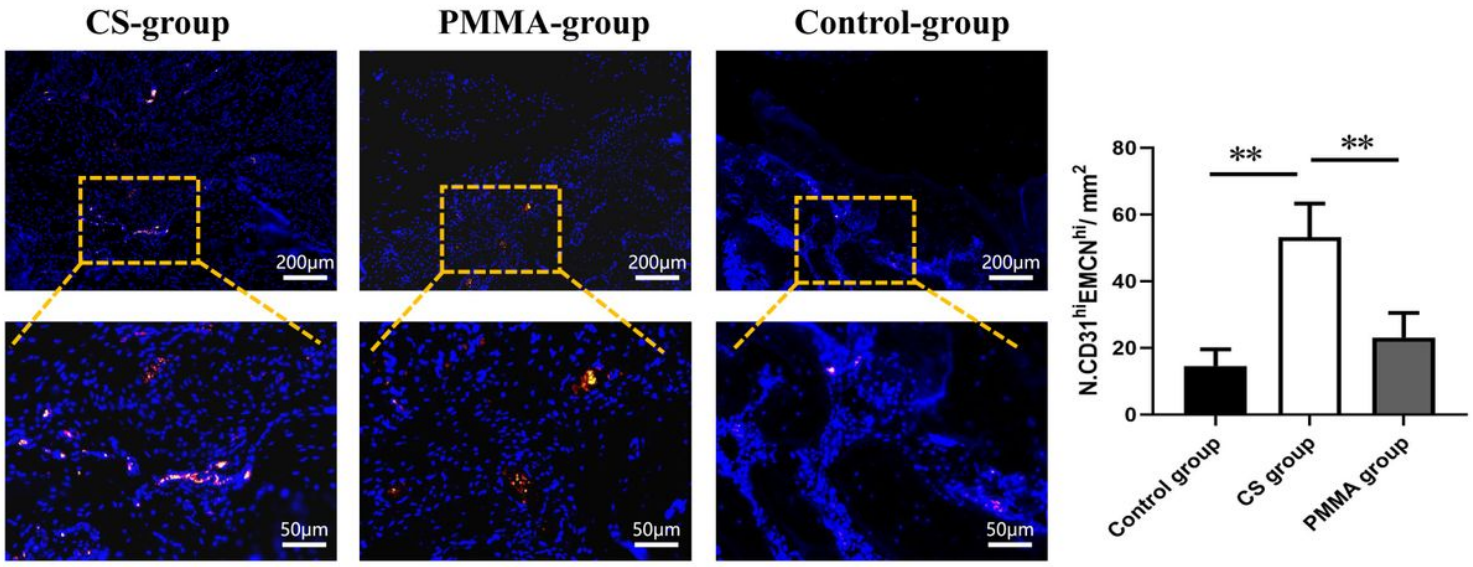

Figure 9

Immunofluorescent staining and quantitative analysis of CD31hiEmcnhi in bone defects area at 20 weeks postoperation. n=5 per group. Scale bar, 200 μm. Magnified view, 50 μm. **p < 0.05 compared as denoted by bar.